University of Groningen

Slowing starch digestibility in foods

de Bruijn, Hanny Margriet

Link to publication in University of Groningen/UMCG research database

CHAPTER 8

Fiber mix addition to wheat-based flatbread delays the appearance of exogenous glucose and its downstream metabolites in plasma of healthy male subjects

Lisa Schlicker
Hanny M. Boers
Christian-Alexander Dudek
Gang Zhao
Arnab Barua
Jean-Pierre Trezzi
Michael Meyer-Hermann
Doris M. Jacobs
Karsten Hiller

ABSTRACT

Background: Food supplementation with a fiber mix of guar gum and chickpea flour represents a promising approach to reduce the risk of type 2 diabetes mellitus (T2DM) by attenuating postprandial glycemia. However, additional metabolic consequences of the addition of this fiber mix require further characterization.

Methods: In a randomized, cross-over study design, 12 healthy, male subjects consumed three different flatbreads either supplemented with 2% or 4% guar gum and 15% chickpea flour each or no supplementation (control). To follow the metabolic fate of flour components, the flatbreads were enriched with ~2% of ^{13}C-labeled wheat flour. Blood was collected at 16 intervals over a period of 360 minutes and investigated by gas chromatography coupled to mass spectrometry (GC-MS).

Results: Non-targeted metabolome analysis revealed that plasma levels of 11 metabolites were significantly altered upon guar gum intake, including fatty acids, ketone bodies, glucose and -related metabolites. Digestion of the flatbread contributed at maximum 50% to the plasma glucose pool. The flatbread-derived fraction of lactate and alanine were 35% and 25%, respectively and was further decreased for the downstream metabolites citrate and glutamate. The contribution of dietary protein to the plasma metabolite pool was significantly lower compared to starch. Based on flux data of central carbon metabolites, guar gum was shown to reduce the exogenous formation of the downstream metabolites of glucose, lactate and alanine, in a concentration-dependent manner, whereas only marginal effects were observed for citrate and glucose-derived glutamate. The overall effect represented by the appearance rates of these ^{13}C-labeled metabolites was strongest for glucose and attenuated for the downstream metabolites.

Conclusion: The postprandial response of the fiber mix propagated from glucose to some downstream metabolites in a delayed and weakened form. Further investigations to explore the health benefits of these exogenous effects are warranted.

Trial registration: The trial was registered at www.clinicaltrials.gov with the registration number NCT01734590 in November 2012.

INTRODUCTION

There is an increasing worldwide prevalence of type 2 diabetes mellitus (T2DM), especially in the Asian population[1]. It is known that moderate lifestyle interventions such as a prudent diet and exercise can help to prevent T2DM[2]. In addition, lowering of the postprandial glucose response may reduce progression from pre-diabetes to T2DM[3-6]. Especially lowering the postprandial glucose (PPG) response of staple foods is worthwhile, because of their widespread and frequent consumption[7]. The two most common carbohydrate-rich staple foods in South Asia are rice and wheat-based flatbreads[8].

In a previous study, we found that supplementation of guar gum and chickpea flour to wheat-based flatbread lowered dose-dependently the postprandial glucose and insulin responses in Indian and Caucasian subjects[9,10]. Guar gum is a water-soluble viscous fiber extracted from *Cyamopsis tetragonoloba*[11,12] and its consumption has been linked to beneficial health effects including reduced blood cholesterol, enhanced mineral absorption and stimulation of short chain fatty acid production[11,13]. It is assumed that the viscosity and gel-forming characteristics of guar gum are responsible for the reduction of the postprandial glucose response[12]. High viscosity causes reduced mixing of digesta which leads to a delayed interaction between enzymes and substrates. Moreover, it was reported that guar gum binds to α-amylase and thus inhibits its enzymatic function[14]. Chickpea flour is rich in high-quality protein and dietary fibers and similar to guar gum, its consumption is considered to lower postprandial glycemia and insulin[15,16]. Consequently, the ingestion of guar gum in combination with chickpea flour results in delayed gastric emptying and reduced rates of starch hydrolysis and subsequent glucose absorption[12,14,17]. But testing for this hypothesis requires information on the dynamics of glucose metabolism considering that the postprandial glucose response is the integrated result of the rate of appearance of exogenous glucose, rate of disappearance of total glucose and the endogenous glucose production in the liver[18]. In a previous study, Boers *et al.*[19] revealed that guar gum supplementation only slightly reduced the rates of exogenous glucose appearance but had substantial effects on the rates of postprandial disposal and endogenous glucose production[19]. This suggests that the addition of the fiber mix not only affects gastric emptying and the digestion process in the intestine, as expected[14], but also impacts other metabolic rates. For this reason, we studied the postprandial metabolism in human subjects who consumed ^{13}C-enriched flatbreads supplemented with different amounts of guar gum.

To this end, we applied stable-isotope assisted metabolomics to monitor the dynamics of several target metabolites that are derived from wheat flour either *via* starch- or protein hydrolysis. On that account, we followed the catabolism of ^{13}C wheat flour and determined the mass isotopomer distributions (MIDs) of twelve ^{13}C-labeled plasma metabolites. The appearance rates of these metabolites were determined based on a

single metabolite ordinary differential equation model. Moreover, a network model was applied to answer the question whether the intervention influences further metabolic rates downstream of glucose. Finally, we performed non-targeted GC-MS based metabolite profiling to reveal effects on the postprandial plasma metabolome.

To our knowledge, this is the first study assessing a comprehensive dataset of metabolome and metabolic flux data on the consequences of the ingestion of guar gum and chickpea flour in human. In contrast to a technique based on dual stable isotope labeling, which enables the determination of the different fluxes contributing to the postprandial glucose level[19], our approach is not limited to one single metabolite. Since U[13]C-labeled wheat flour was used as a tracer in this experimental setup, it was possible to obtain flux information for twelve ^{13}C-labeled central carbon metabolites.

MATERIAL & METHODS

The complete study design including the preparation of the test products has already been described earlier[19].

Subjects

In short, fifteen healthy men were recruited for screening from on existing database of Quality Performance Service Netherlands B.V., Groningen, The Netherlands, a clinical research organization (CRO). Twelve subjects completed the study. For inclusion/exclusion criteria and ethical aspects see Boers et al[19]. The trial was registered at clinicaltrialsgov.com as NCT01734590.

Experimental design

The study used a double-blind, randomized, controlled, full cross-over (within subject) design. Subjects attended the initial screening day followed by 3 test days, at least 1 week apart. Participants were instructed to minimize changes in their habitual diet and activity during the study period and they were not allowed to consume ^{13}C-enriched food (for list see reference[19]). In addition, they also got a standardized evening meal at the CRO. All participants fasted overnight (from 19.30 hours until consumption of the test product) but were allowed to drink water *at libitum*. Because this was a dual labelled isotope study, next to the labelled food, a priming dose of [2]H-labelled glucose was administered as a bolus followed by a continuous infusion of deuterated glucose for 8 h. At 2 h after the start of the infusion each morning at each test day, subjects consumed three freshly made flatbreads with 250 ml of mineral water as breakfast.

Test product and preparation

The flatbread named GG2 contained 2% guar gum, 3% barley flour and 15% chickpea flour, while the so called GG4 flatbread contained 4% guar gum and 15% chickpea flour. The control flatbread was 100% based on wheat flour. Wheat seeds were intrinsically labelled by growing the wheat plants after germination in a labelling facility

under an atmosphere containing $^{13}CO_2$ (>97 atom% ^{13}C). The test products obtained a final ^{13}C-enrichment of approximately 2% atom percent excess (APE). The study was designed to investigate the metabolism of starch-derived metabolites, thus the ratio between the amount of introduced ^{13}C-flour and total carbohydrate content was adjusted in the three conditions control, GG2 and GG4. The treatments were not matched for total protein and amino acid composition.

Sample collection

Blood samples were collected in K_2-EDTA-tubes containing dipeptidyl peptidase-IV (BD Diagnostics) at time points -30, -5, 15, 30, 45, 60, 75, 90, 105, 120, 150, 180, 210, 240, 300 and 360 min and centrifuged at 1300 g for 10 min at 4°C within 30 min after collection to limit pre-analytical variation[20]. Resulting plasma was stored at -20°C prior extraction.

Metabolite extraction from plasma

Prior to metabolite extraction, plasma samples were thawed on ice for 30 min. Extraction was performed in technical triplicates. We combined 20 µl plasma with 180 µl extraction fluid composed of 4 parts of methanol and 1 part of water which contained three internal standards (Pentanedioic acid-d6 (final concentration: 20 µM), U^{13}C-Ribitol (final concentration: 12.7 µM), Norleucine (final concentration: 10 µM)). The mixture was subsequently vortexed at 4°C and 1400 rpm for 5 min and centrifuged at 4°C and 21.000 g for 10 min. After centrifugation, 140 µl of the supernatant were transferred to a glass vial with insert and left-over extract was collected, mixed and used for the preparation of pool samples. All pipetting steps during metabolite extraction were performed by a pipetting robot (Freedom Evo, Tecan Life Sciences, Männedorf, Switzerland). The extracts were dried overnight at -4°C in a refrigerated vacuum concentrator (Labconco, Kansas City, USA) and stored at -80°C prior GC-MS measurement.

Metabolite Derivatization and GC-MS Measurement

Sample derivatization and GC-MS measurement were performed according to Krämer *et al*[21]. Briefly, metabolites were derivatized with 15 µl of 2% methoxyamine hydrochloride in pyridine for 90 min and 15 µl N-methyl-N-trimethylsilyl-trifluoroacetamide (MSTFA) for additional 30 min at 40°C under continuous shaking using a Gerstel MPS.

For GC-MS analysis, an Agilent 7890A GC with a 20 m DB-5MS capillary column (0.18 mm inner diameter, 0.18 µm film thickness) connected to an Agilent 5975C inert XL MSD was used. Details of the GC-MS measurement are provided elsewhere[21].

Data processing

Obtained SIM and SCAN GC-MS data were processed using the software package MetaboliteDetector[22] as described by Krämer *et al*[21].

MID determination

MIDs were determined from the generated SIM data using MetaboliteDetector's sum formular-based MID wizard[19]. For the mass isotopomers of the metabolites glycine, serine, citrate and glutamate, the non-labelled spectra based correction was applied[23].

Batch quantification and normalization

We applied MetaboliteDetector's batch quantification wizard for the relative quantification of the metabolite levels for the obtained SCAN data. Metabolite levels were subsequently normalized to pool samples as specified elsewhere[24].

Data and statistical analysis

The collected SIM glucose data did not allow for accurate MID determination, thus, the glucose M6 data were kindly provided by the Department of Laboratory Medicine, University Medical Center Groningen, University of Groningen, Groningen, The Netherlands. Plasma glucose levels were derived from the collected SCAN data.

Contribution of food-derived metabolites to the total metabolite pool

The maximal contribution of food to the plasma metabolite pool was calculated based on the maximal ^{13}C-enrichments obtained after the consumption of the control flatbread enriched by 2%. We assumed a linear relationship between the ingested and the obtained ^{13}C-enrichment[25]. To determine the contribution of food to the plasma metabolite pool, the obtained enrichment was multiplied by 50 to simulate the ingestion of flatbread enriched by 100%.

Areas under the curve (AUCs)

AUCs$_{0-120}$ for the metabolites levels of glucose, lactate, alanine, citrate and glutamate were calculated with R (version 3.4.4) using the package "DescTools" with the trapezoidal rule to compare the obtained results with Boers *et al*[19].

Outlier analysis

Outliers were identified using principal component analysis (PCA) in SIMCA 15.0 (Umetrics, Umea, Sweden). In the untargeted dataset, 76 out of 1661 measurements were identified as outliers and thus excluded for further analysis. In the MID dataset, 679 (out of 1190 measurements x 115 MIDs = 136850) single data points were excluded.

Repeated Measures (rm)ANOVA

Repeated measures ANOVA (rmANOVA) was performed using R version 3.4.4. For both, the untargeted data set and the MID data set, the analysis was performed on the medians of the technical triplicates on the factors intervention and time and the combination of both. We accounted for multiple testing using the Benjamini & Hochberg p-value adjustment[26].

Statistical analysis of single time points

Analysis of variance (ANOVA) was performed using JMP Pro 14.0.0 (SAS Institute Inc. 2013, Cary, North Caroline, USA). For the untargeted data set, mixed models were built per time point using the fixed factors treatment (Control, GG2, GG4), replicate and baseline (median of triplicate measurement at time points -30 and -5 min) and the random factor subjects. For the MID data set, the same mixed models were built, yet without the fixed factor baseline. Post-hoc multiple comparisons of the LSMeans using a Dunnett-Hsu adjustment were compared to compare the effects of GG2 and GG4 to control, respectively. A value of $p<0.05$ was considered statistically significant.

Metabolic modeling – Single metabolites

We set up a single metabolite model to compute the appearance and the disappearance rates of the labeled metabolites separately. We, thereby, assume that the metabolite is formed from a precursor in a different compartment according to the well-known metabolic pathways, subsequently transported into the blood stream at rate k_1 (appearance rate) and leaving the system at rate k_2 (disappearance rate) upon consumption. E.g. the *metabolite* lactate is derived from the *precursor* pyruvate inside the cell. We assume the pool size of the *precursor* pyruvate to decrease when it is converted to the *metabolite* lactate. The model can be described using the following system of ordinary differential equations (ODEs) (Eq. 1).

$$\frac{dprecursor}{dt} = -k_1 \cdot precursor$$
$$\frac{dmetabolite}{dt} = k_1 \cdot precursor - k_2 \cdot metabolite \quad (1)$$

We used the model described above to compute the appearance rate (k_1) and disappearance rate (k_2) for metabolites that incorporated ^{13}C labeling. For fitting, we used the relative metabolite levels multiplied with the mass isotopomer (MI) abundance specifically enriched from starch or protein hydrolysis in percent resulting in relative amounts of labeling. The parameters of the model are estimated using the Levenberg-Marquardt[27,28] algorithm for least squares curve fitting. To overcome the initial value problem of the method we used a genetic algorithm to solve the system with different, randomly generated initial values. As a result we received a set of optimized parameters with the corresponding root mean square deviation (RMSD) for every run of the genetic algorithm (Eq. 2).

$$RMSD = \sqrt{\frac{\sum(\hat{y}_i - y_i)^2}{N}} (2)$$

The final parameters are the means of the best fitting parameter sets. We used the parameters of the control to compare with the different conditions. To compare the effect size between metabolites, the computed rates for GG2 and GG4 were normalized to the respective Ctrl rate and multiplied by 100 to obtain a percentage.

Metabolic modeling – Network model

$$\frac{dPyr}{dt} = k_1 \cdot c_{Glc} + k_{2b} \cdot L + k_5 \cdot c_{Ala} - \left(k_{2f} + k_3 + k_{d,Pyr}\right) \cdot c_{Pyr}$$

$$\frac{dCit}{dt} = k_3 \cdot c_{Pyr} - \left(k_4 + k_{d,Cit}\right) \cdot c_{Cit}$$

$$\frac{dLac}{dt} = k_{2f} \cdot c_{Pyr} - \left(k_{2b} + k_{d,Lac}\right) \cdot c_{Lac} \qquad (3)$$

$$\frac{dGlu}{dt} = k_4 \cdot c_{Cit} - k_{d,Glu} \cdot c_{Glu}$$

where *c* represents the metabolite concentrations (pyruvate M3 (excluded from the fitting process due to low quality of pyruvate measurement), citrate_M2, lactate_M3, glutamate_M2, glucose_M6 and alanine_M3), *k* represent the rates of the network and k_d represents the outgoing fluxes. Glucose M6 and alanine M3 were interpolated from data and treated as input to the model (**Fig. 7**).

The model was fitted to individual subject data in two scenarios. Firstly, assuming that the rate constants in the model were not changed by the interventions, the model was fitted to the control, GG2 and GG4 data simultaneously. The quality of the fit here serves as a baseline, referred to as Model 1 (M1) in the following, to compare the results from the other scenario to. In the second scenario, one of the six rate constants was assumed to be influenced by the intervention and thus takes different values for the control, GG2 and GG4 in the fitting procedure (referred to as Model 2 (M2) to Model 7 (M7) in the following). Please note that the simulated quantities are in principle concentration in cells, which are assumed to be proportional to the blood compartment from which the samples were collected. Therefore four scaling factors, connecting cellular levels to blood levels, were included as free parameters in the fitting procedure. The fitting procedure was guided by minimizing the root mean square difference between model simulation (y) and the measured data points (ŷ).

$$RMS = \sqrt{\sum \frac{(y_i - \hat{y}_i)^2}{\sigma_i^2}} \quad (4)$$

where *σ* denotes the standard deviation of the measured data point, and *n* denotes the number of data points.

A differential evolution based global optimizer was employed for fitting. We allow a large parameter space for the rate constants while the scaling factors are limited in their physiological range. Each optimization task was repeated 50 times, among which the best result was used to calculate the Akaike information criterion with correction (AICc)[29] for model comparison (Eq. 5). The AICc evaluates model quality based on both quality of fitting and the number of free parameters. 2 units larger in AICc means 0.368 times as probable as the model having smaller AICc.

$$AICc = 2P + RMS^2 + N log(2\pi) + 2\frac{P(P+1)}{N-P-1} \quad (5)$$

where P is the number of fitted parameters, N is the number of data points.

RESULTS

Postprandial effects of Sharbati flour flatbreads on metabolite levels

To measure the postprandial metabolite profiles in plasma, we extracted plasma metabolites at 16 timepoints from volunteers who ingested Sharbati flour flatbreads and performed a non-targeted GC-MS analysis.

Based on the mass spectrometric measurement, we detected at total 380 plasma metabolites in the plasma of the 12 studied persons. Using repeated measures ANOVA (rmANOVA, $p < 0.05$), we found a total of 100 metabolites showing significantly altered levels in the postprandial phase (Supp. Fig 1). We were able to identify 32 of the detected metabolites. Their time-resolved levels are depicted in **Fig. 1.** As expected, the abundance of most metabolites increased within the first hour after food intake reaching a maximum between 45 and 60 minutes. Among those compounds were amino acids (such as phenylalanine, threonine, serine, tyrosine, glutamine, isoleucine, valine, glutamate, lysine, proline and glycine) and carbohydrate related metabolites (such as glucose, fructose and gluconic acid). In contrast, the levels of alanine and lactate started to increase at later timepoints and reached their maximum only 75 minutes post ingestion. After 360 minutes, the levels of most metabolites decreased either back to or even below their baseline concentration. In contrast, the levels of a few metabolites including 3-hydroxybutyrate, palmitate, stearate and octadecenoate declined directly after flatbread intake and reached a minimum between 105 and 150 min. This was expected as these metabolites are synthesized by adipose tissue and the liver under fasting conditions[30]. Interestingly, all these levels increased to twice their baseline levels after 360 min. Taken together, we observed increased levels of metabolites derived from food catabolism while the amounts of endogenous energy metabolites such as ketone bodies and fatty acids were decreased directly after food intake. This is in line with previous studies and validates our clinical and experimental setup[31–34].

Incorporation of ^{13}C enrichment from 2% labeled wheat flour in central carbon metabolites

Next, we aimed to study to which extent plasma metabolites are derived from the ingested flatbread during digestion and catabolism. Due to the continuous turnover (appearance and disappearance) of plasma metabolites, the fraction of food derived metabolites cannot be determined based on time-resolved concentration changes alone. To reveal metabolic fluxes through pathway metabolites, stable-isotope labeling can be applied. The metabolic conversion of stable-isotope labeled compounds is almost identical to that of the respective unlabeled analogue, however, the molecular masses of the compound itself and of all downstream metabolites are increased and can thus be distinguished by mass spectrometry. A low amount (2%) of the wheat flour was substituted with fully ^{13}C-labeled wheat flour to prepare the flatbread. Because of the isotope incorporation, downstream metabolites can be traced and their isotopic

enrichment can be quantified. Wheat flour is composed of approximately 63-72% starch and 12% protein[35] both of which are hydrolyzed by amylases and proteases in the gastrointestinal tract (GIT) resulting in the release of glucose and free amino acids into the blood. To detect flour derived ^{13}C isotopes in these metabolites, we applied a specific GC-MS based workflow, especially developed for the sensitive detection of very low ^{13}C-enrichments[21]. Since the initial enrichment in the wheat flour was only 2%, and mixing with endogenous plasma metabolites causes further dilution, we expected very low isotope enrichments in plasma metabolites. We were able to detect and quantify ^{13}C-enrichment in 12 central carbon metabolites, specifically glucose, serine, glycine, lactate, alanine, citrate, glutamate, glutamine, threonine, tyrosine, lysine and isoleucine. It is apparent that essential amino acids such as lysine and isoleucine can only be derived from protein hydrolysis whereas carbohydrates such as glucose can only be derived from starch hydrolysis. On the other hand, several intermediates of central carbon metabolism can originate from both sources. As an example, serine can be catabolically provided by protein hydrolysis or anabolically by endogenous amino acid synthesis. Both pools, anabolic and catabolic, are mixed in the blood and can in most cases not be distinguished. **Figure 2** depicts the atom transitions for the conversion of starch derived glucose via glycolysis and the tricarboxylic acid (TCA) cycle as well as the appearance of the free amino acids after protein hydrolysis. The stable-isotope labeling allows for pinpointing to the origin of some metabolites. Glutamate or glutamine are either directly derived from protein hydrolysis or from starch hydrolysis and subsequent TCA metabolism of glycolytic acetyl-CoA. In the first case, all 5 carbon atoms will be ^{13}C enriched and produce M5 isotopologues if labeled wheat protein is hydrolyzed. In the second case, only two carbon atoms will be replaced by stable-isotopes and produce M2 isotopologues (**Figure 3**). In our dataset, glucose, lactate, citrate (M2) and glutamate (M2) originate from starch while glutamine, glutamate (M5), threonine, tyrosine, lysine and isoleucine, originate from wheat protein. The amino acids serine, glycine and alanine can either originate from starch *via* glycolysis or from protein hydrolysis, both pathways will result in identical isotopologues. After ingestion of the flatbread prepared from 2% ^{13}C enriched flour, we observed a maximum of 1% isotopic enrichment in plasma glucose. The observed enrichment of downstream metabolites decreased with increasing distance of the respective metabolite to glucose in the metabolic network. At maximum, 0.6% of the lactate and 0.5% of the alanine pool were labeled from the 2% enriched flour, indicating that a significant fraction of glycolytic intermediates is fueled by the food product. Intriguingly, we robustly detected starch derived enrichment even in metabolites linked to the TCA cycle such as citrate and glutamate. Due to mixing with endogenous metabolite pools, we only found 0.4% and 0.2% isotopic enrichment, respectively. Interestingly, protein hydrolysis only contributed to a quite low extent to most amino acid pools and the isotopic enrichment was below 0.2% for most of them. The only exceptions were the essential amino acid isoleucine with a labeled fraction

of 0.4% and the glycolysis-derived amino acids alanine, serine and glycine with maximal enrichments of 0.5%, 0.15% and 0.2%, respectively. However, in the case of alanine, glycine and serine, labeling from starch and protein hydrolysis can mix and explain the higher enrichments in these metabolites. Based on the observed isotopic enrichments, we calculated the maximal total contributions of the food product to the respective plasma metabolite pool (**Table 1**). The lower enrichment in plasma amino acids compared to starch derived metabolites reflects the composition of wheat flour[35].

The non-essential amino acids alanine, serine and glycine can either be indirectly synthesized from glucose *via* glycolysis and transamination or directly *via* hydrolysis of wheat protein. Based on the profiles of their appearance, the main origin of these amino acids can be estimated. The kinetics of alanine appearance was more similar to that of lactate, suggesting that alanine was primarily derived from starch hydrolysis. In contrast, the profiles of serine and glycine were characterized by an earlier T_{max} and lower maximum enrichment, thus, we hypothesize that protein hydrolysis was the main contributor to serine and glycine formation.

The maximal enrichment obtained for the plasma metabolites is determined by different factors, most importantly the amount of labeling introduced into the system and the size of the non-labeled metabolite pool. The most frequent amino acid found in wheat gluten is glutamate with a relative abundance of 31 mol% (2450 µmol/g)[36]. Since the non-labeled glutamate pool in blood is rather small (61 µM, Source: HMDB), we expected to observe the highest maximal enrichment of all analyzed amino acids for glutamate. Surprisingly, we only measured a very low maximal enrichment for glutamate (0.0665%) as compared to the other amino acids. However, the highest maximum enrichment was obtained for isoleucine (0.4151%), although the relative abundance of this amino acid in wheat gluten protein is only 4.1 mol%[36] whereas its plasma concentration is similar to that of glutamate (69 µM, Source: HMDB). Based on these observations, we conclude that the turnover of glutamate is significantly higher than that of isoleucine. This observation is in agreement with the important role of glutamate for whole body ammonium homeostasis[37,38]. In contrast to essential branched chain amino acids, which are mainly prone to catabolism and feed into the TCA cycle for energy supply[39], glutamate and glutamine are cellular sinks for amino groups and are thus endogenously synthesized and secreted to the blood stream for further hepatic processing[40].

Intervention effects of GG2 and GG4

After having determined the baseline of postprandial metabolism of chapati bread, we aimed to study whether guar gum and chickpea flour as food supplements induces changes in postprandial metabolism. For this purpose, 2% and 4% of guar gum (GG2, GG4) in combination with 15% chickpea flour were blended in the chapati formulation. We, then, determined the postprandial levels of the plasma metabolite.

In general, the impact of the fiber mix supplementation on plasma metabolite levels was only moderate when compared to their baseline profiles. We observed a reduction in the postprandial glucose level (**Fig. 3**), its maximum level after 45 minutes was reduced by ~ 6% in case of GG4 and by 5% in case of GG2. In addition, we found a significant reduction of the maximum amounts of fructose (GG2: -13%, GG4: -6%), gluconic acid (GG2: -5%, GG4: -22%) and two unidentified metabolites (RI 2028: GG2: -6%, GG4: -12; RI 1958: GG2: -11.6%, GG4: -11.4). The free fatty acids palmitate, stearate and octadecenoate, as well as the ketone body 3-hydroxybutyrate were increased in response to the supplementation (**Supp. Fig. 2**), most probably as a consequence of a reduced glycemic effect. The levels of 2-hydroxybutyrate, a biomarker for insulin resistance[41] and a metabolite of threonine catabolism, were increased in a dose-dependent manner (**Supp. Fig. 2**). Beyond that, we did not detect further significant effects on the levels of other downstream metabolites of glucose (**Fig. 3**).

Next, we set out to analyze whether the combination of guar gum and chickpea flour affects metabolic fluxes and turn-over rates of wheat-derived metabolites through their respective plasma pools. **Fig. 4** depicts the response curves of the ^{13}C-enriched metabolites for control, GG2 and GG4, respectively. In contrast to the plasma metabolite levels presented in the previous section, due to the isotope labeling these graphs do exclusively highlight the parts of the plasma pools that are food derived.

We observed significant effects of GG2 and GG4 on the appearance and disappearance of most analyzed metabolites. The response of glucose M6 isotopologues was significantly attenuated by GG2 and GG4. GG2 and GG4 delayed T_{max} by 30 and 60 min, respectively, and reduced the maximal ^{13}C-enrichment by ~ 6% for GG2 and GG4. In contrast to their pool sizes, ^{13}C enrichment profiles of lactate and alanine were indeed significantly altered due to the fiber mix addition. In line with the dynamics of glucose M6, the formation of lactate M3 and alanine M3 was delayed by 60 min following ingestion of GG4, but not GG2. The maximal ^{13}C enrichment of lactate M3 was reduced by 11% and 13%, for GG2 and GG4 respectively and for alanine M3, we observed a reduction by 13% and 17%, respectively. These results additionally support our previous results that alanine is primarily formed from glucose in the postprandial phase. The effects observed for glucose M6, lactate M3 and alanine M3 were less pronounced in the glucose derived M2 isotopologues of citrate and glutamate (see **Fig. 2** for atom transitions and isotopologue formation). Due to the increasing metabolic distance of these metabolites to the tracer, we found the maximal enrichment of these metabolites only 300 to 360 minutes after bread ingestion. In addition, the maximal fraction of citrate and glutamate M2 isotopologues tended to be reduced by GG2 and GG4 respectively, yet without statistical significance. Similar to citrate and glutamate M2, rmANOVA did not reveal a statistically significant

intervention effect on the profiles of serine M3 and glycine M2 isotopomers, indicating that the formation of these metabolites is not primarily fueled by postprandial glucose.

Based on the obtained data, we observed an intervention effect for the protein-derived amino acids glutamate M5, glutamine M5, valine M5 and tyrosine M9 as well (**Supp. Fig. 3**). Similar to the starch-derived metabolites, the maximal ^{13}C-enrichment was reduced in a concentration-dependent manner, however, we did not observe a delay in T_{max}. As the study was designed to investigate primarily starch hydrolysis and its downstream metabolism, the protein content and composition was not adjusted. Thus, we cannot know whether the observed effect is induced by the intervention or by the different protein contents and compositions.

Taken together, our results indicate that GG4 ingestion caused a significant postprandial delay of starch hydrolysis that propagated to its glycolytic downstream metabolites glucose, lactate and alanine, but was less pronounced in TCA cycle intermediates. When comparing the metabolite levels and the ^{13}C-enrichment profiles, it must be noted that the postprandial metabolite levels return to baseline within a six hour time frame, while the labeling remains in the system for a longer period of time, pointing to a fast adjustment of endogenous metabolite fluxes to the food intake.

Modeling approach

The combination of the time-resolved data on metabolite levels and MIDs allows for the determination of metabolic turnover rates comprising information on postprandial kinetics and how they are affected by the interventions. We followed two different modeling approaches; an ODE-based independent single metabolite model and a metabolic network model.

The single metabolite model was used to compute metabolite-specific appearance rates. This could only be done for metabolites that exhibited detectable incorporation of ^{13}C atoms. As the metabolic conversions are taking place inside of cells, we assume that the precursor metabolite is converted within the tissue and transported into the blood stream at rate k1. The metabolite is disappearing from the blood stream at rate k2. We used the relative amounts of labeling to fit the data and computed the respective appearance rates (**Suppl. Table 1**). For the starch-derived metabolites, meaningful disappearance rates could not be computed because the profiles did not return to zero during the time range of blood collection. GG4 induced a significant reduction in the appearance rate of glucose, similar trends were observed for lactate and alanine (**Fig. 5 a**). For citrate, glutamate, serine and glycine, this effect could not be observed. To determine how the effect of guar gum and chickpea flour propagated downstream of glucose, we calculated the effect size for all starch-derived metabolites by normalizing the rates of GG2 and GG4 to the control rate (**Fig. 5 b**). While the appearance rate of glucose was reduced by 20% and 38% following GG2 and GG4 ingestion, the effect size was decreased for lactate (GG2: ~9%, GG4: ~12%) and

alanine (GG2: ~5%, GG4: ~15%). For citrate and glutamate, the values obtained for GG2 and GG4 did not differ from those obtained for the control. These results indicate that the effect on the overall appearance induced by the fiber addition was strongest for glucose and was attenuated downstream of glucose. Moreover, the observed effect was strongest for GG4 suggesting that the effect size is dependent on the amount of ingested guar gum.

Using a metabolic network model, we addressed the question whether the effects induced by the interventions primarily follow the effect observed for glucose or if there are additional glucose-independent effects for the glucose-derived metabolites. Due to the strong inter-individual variation, these effects were addressed for each subject separately. To this end, we designed a simplified model of central carbon metabolism to describe the generated data. The model was based on glucose, pyruvate, lactate, alanine, citrate and glutamate (**Fig. 6a**). Glucose and alanine data were used as input to the model. Seven different models were generated. In model 1, all rates were fixed not allowing for any flexibility for intervention induced changes on any glucose-derived metabolites, and then model parameter were fitted to the data. For the other models (2-7), a single rate per model was left flexible and the parameters were fitted again. As a quality measure, the Aikaike Information Criterion corrected for small sample sizes (AICcs) were calculated for each model and subject separately. For better comparison, the obtained AICcs were normalized to the AICc obtained for model 1 (**Fig. 6b**). Assuming that the interventions induced similar changes to downstream metabolites as to glucose, model 1 should describe the data best. In case the interventions would impact downstream rates independently, as for example the conversion from pyruvate to lactate, model parameter will better fit with k_{2f} kept flexible and thus resulting in lower AICcs. Lower AICcs are in this case a measure of better modeling quality. We observed inter-individual differences in the AICc profiles (**Fig 6b**). For subjects 4 and 9, the interventions did not have additional effects when compared to the kinetics of glucose. However, for the other subjects, the fitting quality was strongly increased when the rates k_{2b}, k_{2f} or k_3 were flexible, indicating that the intervention induced changes on the conversion rates of downstream metabolites that were independent of the kinetics of glucose appearance.

Based on the modeling approaches, we found that the intervention had the strongest effect on glucose appearance which was attenuated to downstream metabolites. The metabolic network model revealed that the kinetics of the downstream metabolites were dependent on the individuals and that they did not just follow the kinetics of glucose for most subjects. This suggests that the interventions induced effects on the downstream metabolites lactate, alanine, citrate and glutamate that were independent of the glucose kinetics. The findings obtained from the different modeling approaches complement each other in a way that the attenuation in the appearance rates of the

downstream metabolites could be reflected by the glucose-independent effects identified by the network model.

DISCUSSION

In this study, we first assessed postprandial metabolic effects caused by flatbread ingestion without any intervention (control). For that purpose, we studied postprandial metabolite levels and applied *in vivo* stable-isotope labeling to analyze turn-over rates of plasma metabolites. We then used this information as the basis to determine the impact of guar gum supplementation on the postprandial response.

Using non-targeted GC-MS based metabolite profiling, we found that the levels of 100 out of 380 detected metabolites in plasma were significantly altered over the course of the 360 minute postprandial interval. 45-60 minutes after flatbread intake, mainly carbohydrate-related metabolites (glucose, fructose, gluconic acid) and amino acids were increased due to the hydrolysis of starch and proteins present in the flatbread[34]. In contrast, concentrations of free fatty acids such as stearic acid and palmitic acid as well as the level of the ketone body 3-hydroxybutyrate first decreased within in the first 210 minutes, likely due to insulin dependent inhibition of lipolysis and then strongly increased due to insulin depletion[30,34,42]. These metabolite profiles are in accordance with other studies and reflect the absorptive and the post-absorptive phase after food ingestion[31–34].

The consumption of fully ^{13}C-labeled wheat flour rather than a single ^{13}C-labeled compound provides deep insights into the kinetics of the digestive processes of the major constituents of wheat flour. By employing our recently published GC-MS based workflow for the detection of low isotope enrichment in ^{13}C-labeled metabolites[21], we were able to quantitatively follow starch-derived isotopes through starch hydrolysis subsequent glycolysis and TCA cycle metabolism down to glutamate. To our knowledge, this is the first study that simultaneously assessed the postprandial kinetics of glucose and further downstream metabolites upon ingestion of labeled wheat bread in human. Comparable studies are either based on single tracers instead of fully ^{13}C-labeled food products and/or focus on the kinetics of single metabolites, most commonly glucose[18,40,43,44]. In addition, based on the generated data, we could quantify the contributions of exogenous and food-derived metabolite fractions to their total metabolite pools in plasma. At the time point of maximal ^{13}C enrichment, 50% of the total glucose pool, 35 % of the total lactate pool and 25% of the total alanine pool was food-derived. The contributions of food-derived citrate (21%) and glutamate (12%) were further reduced, indicating that reduction of maximal ^{13}C-enrichment is dependent on the metabolic distance to glucose. In contrast, only 3-4% of hydrolyzed wheat protein contributed to the total metabolite pools of glutamine and glutamate confirming that the majority of these compounds are endogenously produced in such a case[40].

The maximal enrichment of protein-derived amino acids was generally lower due to the lower fraction of protein (12%) in the wheat flour as compared to that of starch (77%)[35]. Surprisingly, of all detected protein-derived amino acids, isoleucine showed the highest ^{13}C-enrichment (0.4%), indicating that almost 20% of the isoleucine pool derived from the flatbread. This observation was not expected since glutamate and proline are the most abundant amino acids in the wheat protein gluten[36]. However, Adibi and Gray have shown that isoleucine has one of the highest intestinal absorption rates while glutamate has one of the lowest after *in vivo* perfusion of the jejunum of humans with equimolar amino acid mixes[45,46]. In addition, it was reported that essential amino acids are more efficiently absorbed as compared to non-essential amino acids[47]. We therefore conclude that next to the amount of introduced labeling and the non-labeled pool size, the different absorption efficiencies of dietary amino acids have a major influence on the maximum ^{13}C-enrichment.

Supplementation of guar gum and chickpea flour altered the levels of 11 out of 380 detected metabolites (including glucose) indicating that the intervention induced only minor changes in the plasma metabolome. The AUC_{0-120} of total glucose was significantly reduced upon ingestion of GG4 which is in line the results of Boers *et al.*[19]. Interestingly, the levels of the downstream metabolites lactate and alanine were not affected by the intervention. Based on the response curves of the ^{13}C-enriched metabolites on the other hand, we found that the exogenous appearance of not only glucose but also lactate and alanine was significantly reduced at T_{max}. For lactate and alanine, we observed stronger effects for GG4 (13-17% reduction) than for GG2 (11-13% reduction) showing that the dose-dependent effect of guar gum reported on glucose[19], holds true for lactate and alanine as well.

We applied modeling-based approaches to further explore intervention-induced effects and how these are related between the investigated intermediates. Only by looking at the response curves of the enriched metabolites, we observed that the reduction in the maximal enrichment was stronger for lactate and alanine as compared to glucose. However, for the computation of appearance rates, the plasma metabolite levels were taken into account and provide evidence that the effect induced by the fiber mix is attenuated downstream of glucose. In addition, we chose a network-based modeling approach to more closely investigate the *in vivo* situation and the resulting metabolic fluxes[48,49]. Based on the available data, we chose a rather simple description of central carbon metabolism. The network model revealed that the downstream metabolites do not follow the kinetics of glucose. Both approaches provided the results that the kinetics of the downstream metabolites are different from those of glucose due to the attenuation of the guar gum induced effect.

The plasma level of a metabolite is the net result of exogenous production, endogenous production and consumption[18]. By using a labeling strategy based on two

stable isotope tracers, Boers *et al.*[19] demonstrated that the rate of appearance of exogenous glucose was slightly decreased, but the intervention additionally resulted in a reduced rate of endogenous glucose production and glucose disposal resulting in lowered glucose levels[19]. The generated data confirm that the formation of exogenous glucose is decreased following the intervention. However, based on our data, we cannot directly draw conclusions on endogenous production and disposal. Nevertheless, these processes need to be adjusted *in vivo* in order to maintain the observed unaffected plasma levels of lactate and alanine. Since the appearance of exogenous lactate and alanine was reduced, we conclude that the intervention promotes increased endogenous production and/or reduced disposal of lactate and alanine in order to maintain constant metabolite levels (**Fig. 3**). In addition and in contrast to glucose, the exogenous contribution to the metabolite pools of lactate (35%) and alanine (20%) is smaller and therefore, the effect of guar gum might be counterbalanced more easily for lactate and alanine.

Based on the mechanism of action proposed for guar gum hindering the hydrolyzing enzyme α-amylase to access their substrates[12,14], we expected to see an effect on protein hydrolysis as well. Similar to enzymatic starch hydrolysis, the hydrolysis of proteins is based on proteases that need to directly interact with the protein to catalyze hydrolysis. The obtained data could not answer this question finally, thus, further investigation is required to elucidate the effects of guar gum and chickpea flour on protein hydrolysis and subsequent absorption of amino acids in human[50–52].

One limitation of the presented study is that only a minor fraction of wheat flour was substituted with its labeled counterpart. Higher fractions (>2%) would have increased the number of detectable labeled plasma metabolites. In this context, the enrichment in M3 glucose, a marker for gluconeogenesis[53], is of high interest, but did not exceed the limit of detection. Higher amounts of ^{13}C-labeled wheat flour would, thus, extend the size of the metabolic network and metabolic fluxes could be resolved in more detail. Nevertheless, the application of stable isotope-assisted metabolomics in combination with metabolic profiling resulted in a comprehensive data set.

Conclusions

We demonstrated that flatbread digestion and catabolism mainly fuel plasma glucose, while for its downstream metabolites lactate, alanine, citrate and glutamate, the contribution from exogenous sources is diluted as a function of their metabolic distance to glucose. This demonstrates that the major flux of flatbread nutrients towards tissues is mediated mainly *via* glucose, whereas downstream metabolite pools are only indirectly fueled by tissue sources upon glucose conversion. A guar gum intervention not only delayed glucose kinetics, but also attenuated the formation of lactate and alanine from exogenous sources. Furthermore, we demonstrated that the exogenous contribution and utilization of the investigated plasma amino acids

strongly varies reflecting their different functions in human metabolism. Based on the comprehensive data set generated in the course of this study, we conclude that the main effect induced by the intervention manifests in glucose. Thus, the addition of fiber mixes to wheat-based flatbread could represent a promising strategy to lower postprandial glycemia following the consumption of wheat-based flatbreads and further investigations regarding the potential health benefits are warranted

Ethics approval and consent to participate

Ethical approval was obtained from the Medical Ethics Committee of the 'Beoordeling Ethiek Biomedisch Onderzoek' Foundation (Assen, The Netherlands). Each participant provided written informed consent for the study.

Availability of data and material

The data presented in this study are available from the corresponding author on reasonable request.

Competing interests

HMB and DMJ are employees of Unilever, which manufactures and markets consumer food products, including the flour used for the flatbreads in this study.

Author's contributions

DMJ and KH conceived the experiment. HMB was involved in designing the study. LS performed metabolite extraction, GC-MS measurements and data analysis. LS, JPT and DMJ conducted statistical analysis. CAD, GZ, AB and MHH performed modeling. LS, HMB, DMJ and KH wrote and revised the manuscript. All authors read and approved the content of the final manuscript.

Table 1. Maximal contribution of food-derived metabolite to the overall plasma pool - Calculations are based on the obtained enrichment after ingestion of 2% labeled wheat bread multiplied by 50 to simulate 100% ^{13}C-enriched

Isotopomer	Obtained ^{13}C-enrichment at T_{max} after bread ingestion [%]	Maximum food contribution to plasma metabolite pool [%]
Glucose M6	0.9758	48.79
Lactate M3	0.7360	36.80
Alanine M3	0.5075	25.375
Citrate M2	0.4228	21.140
Glutamate M2	0.2428	12.140
Serine M3	0.1384	6.920
Glycine M2	0.1808	9.040
Threonine M4	0.1148	5.740
Valine M5	0.1800	9.00
Tyrosine M9	0.1911	9.555
Isoleucine M6	0.3935	19.675
Glutamine M5	0.0734	3.670
Glutamate M5	0.0704	3.520
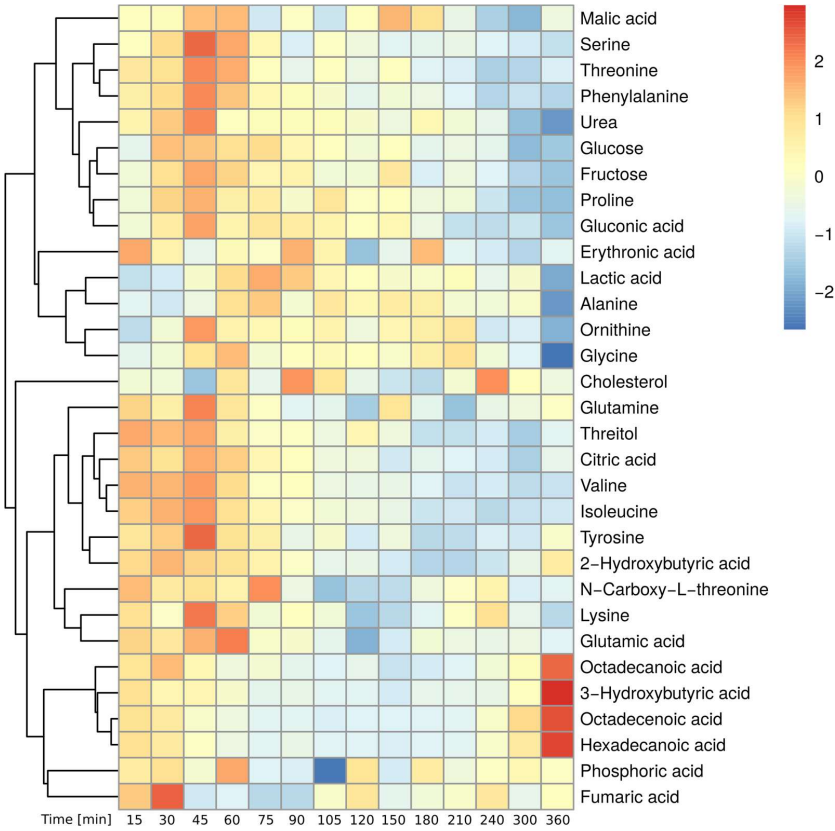
Figure 1: Postprandial effect of wheat bread intake – Heatmap of identified, significantly changed metabolites over time (Median of all subjects, Baseline correction, zScore Normalization)

a)
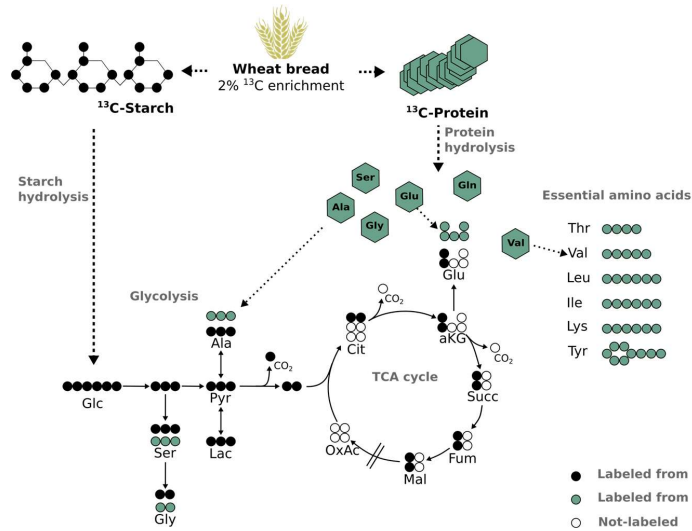
b)
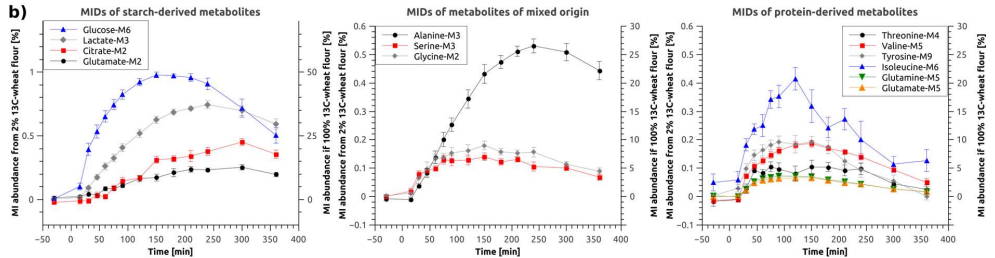
Figure 2: a) Scheme of wheat bread digestion (starch and protein hydrolysis) and atom transitions for metabolic conversions of glucose *via* glycolysis and TCA cycle; b) Time-resolved mass isotopomer (MI) abundances of starch-derived (left) and protein-derived (right) metabolites and metabolites of mixed origin (middle) – Average of all subjects ± Standard Error; Glc – glucose, Ser – serine, Gly – glycine, Pyr – Pyruvate, Ala – alanine, Lac – lactate, Cit – citrate, aKG – α-ketoglutarate, Succ – succinate, Fum – fumarate, Mal – malate, OxAc – oxaloacetate, Glu - glutamate
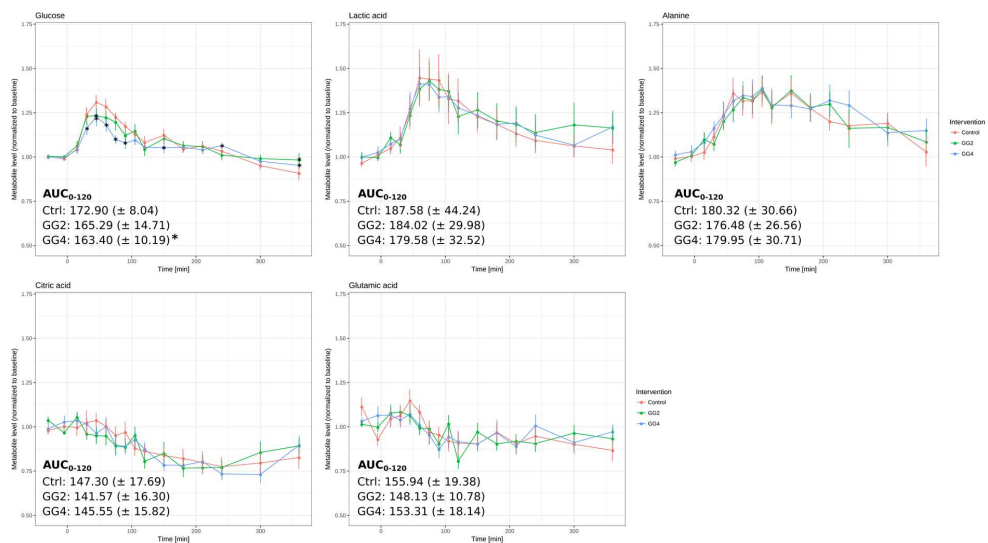
Figure 3: Relative metabolite levels over time and areas under the curve (AUCs) from 0 to 120 min for glucose, lactic acid, alanine, citric acid and glutamic acid (Red – Control, Green – GG2, Blue – GG4; metabolite levels normalized to baseline ± standard error, * indicates significant differences in relation to Ctrl)
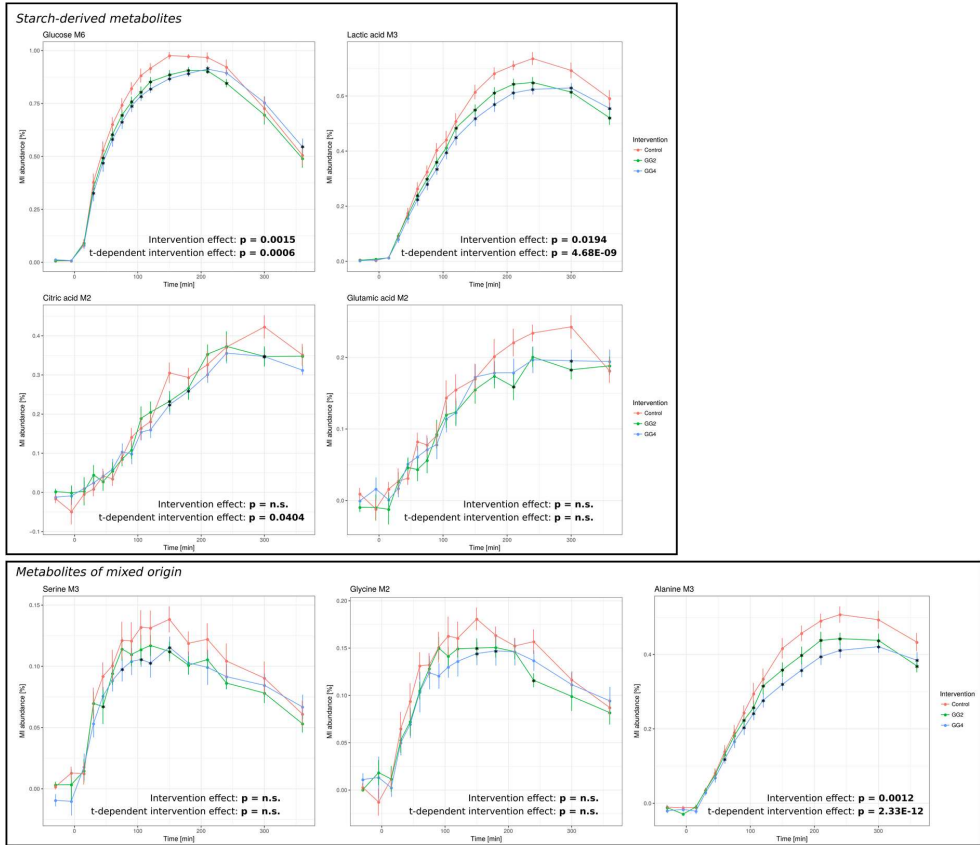
Figure 4: Response curves of ^{13}C-enrichment profiles over time upon intervention for glucose M6, lactate M3, citrate M2, glutamic acid M2, serine M3, glycine M2 and alanine M3 (Red – Control, Green – GG2, Blue – GG4; Average of MI abundance in % ± standard error of 12 subjects; upper box – starch-derived metabolites, lower box – metabolites of mixed origin)
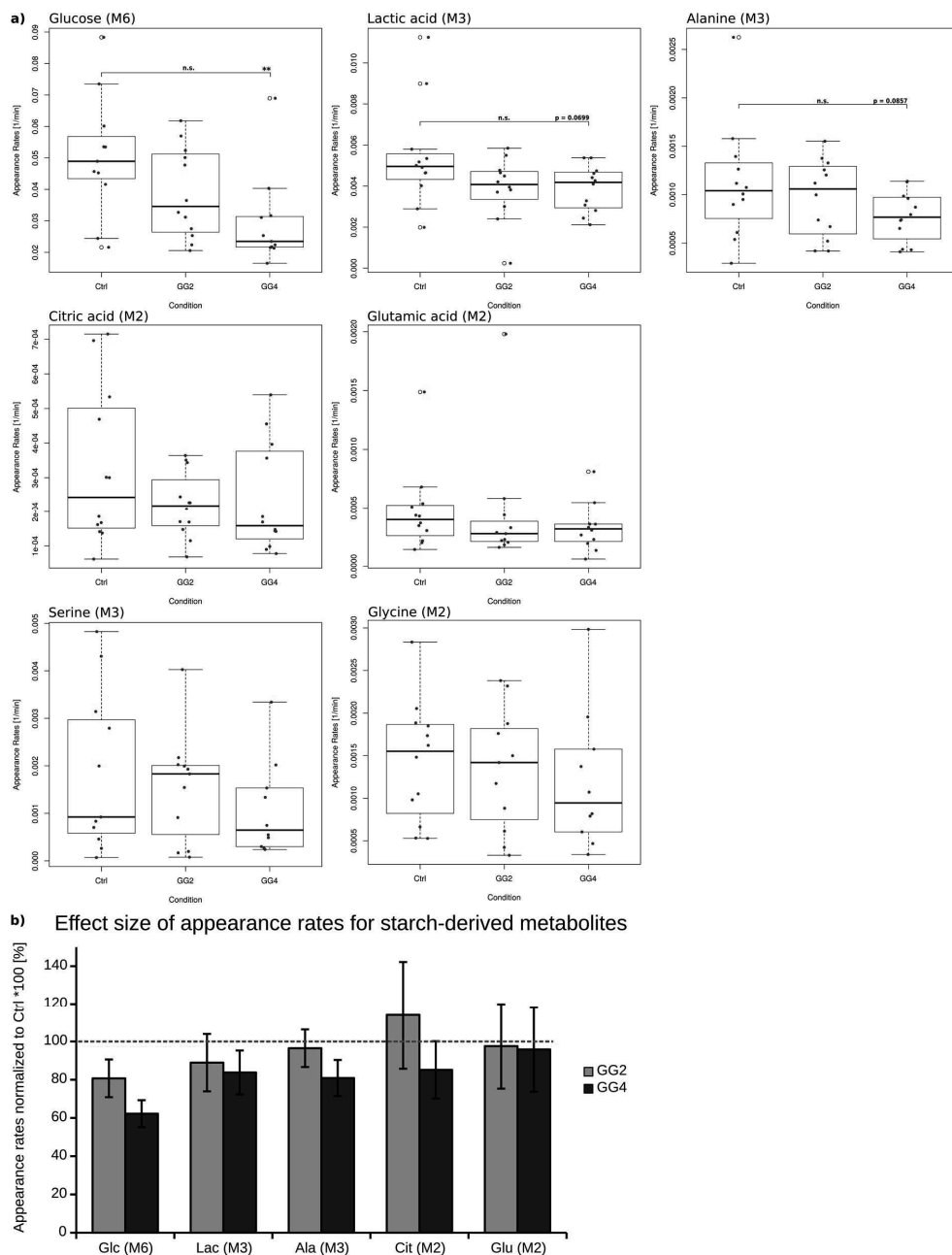
Figure 5: a) Boxplots of modeled appearance rates for glucose M6, lactate M3, alanine M3, citrate M2, glutamate M2, serine M3 and glycine M2 with single data points in blue; b) effect size of the appearance rates of glucose M6, lactate M3, alanine M3, citrate M2 and glutamate M2 by normalization of the appearance rates of GG2 and GG4 to the respective control; average of 12 subjects ± standard error; red dashed line represent 100% and thus, no differences between control and intervention
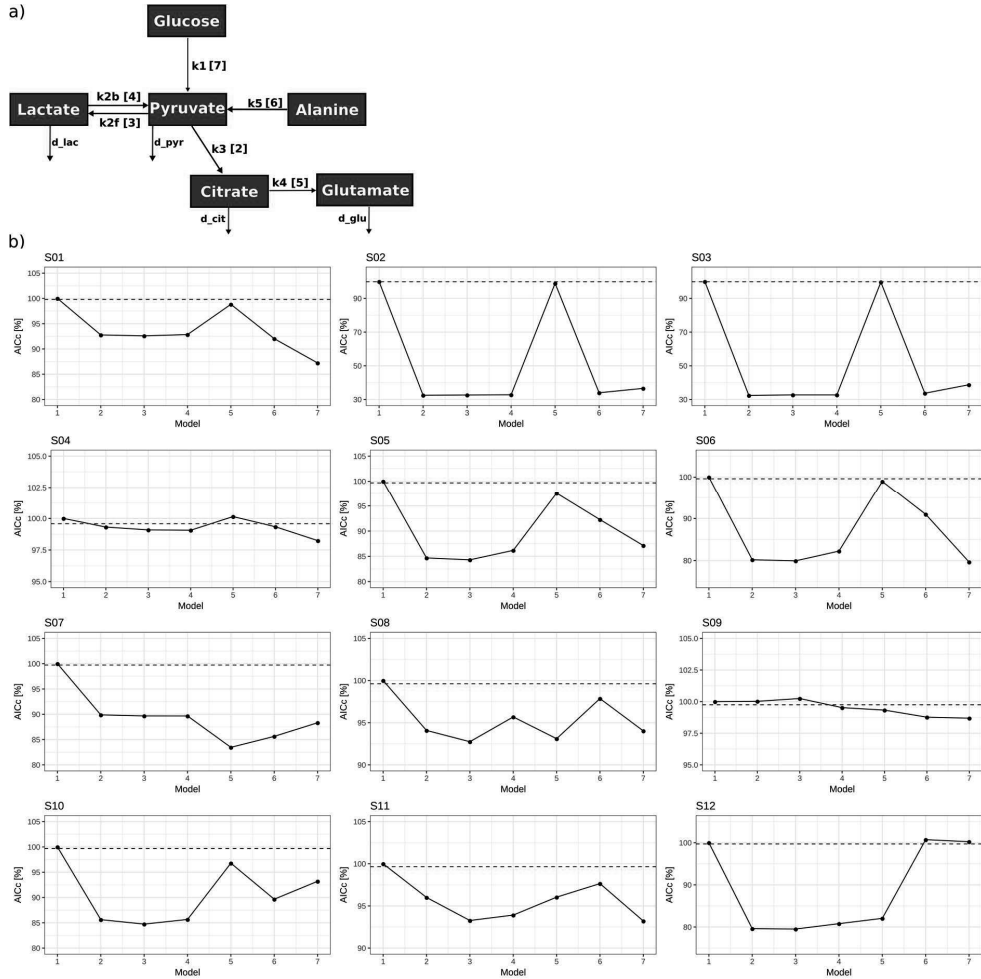
Figure 6. a) Network model connecting the metabolites glucose, pyruvate, lactate, alanine, citrate and glutamate; b) AICcs calculated for the 7 different models (indexed in a) and normalized to the AICc obtained for Model 1 (all rates fixed) for all 12 subjects separately, blue dashed line indicates significantly decreased AICc compared to Model 1

REFERENCES

1. Hu, F. B. Globalization of diabetes: the role of diet, lifestyle, and genes. *Diabetes Care* **34,** 1249–57 (2011).
2. Aakko Uomilehto, J. T. *et al.* Prevention of type 2 diabetes mellitus by changes in lifestyle among subjects with impaired glucose tolerance. *N Engl J Med* **344,** (2001).
3. Chiasson, J.-L. *et al.* Acarbose for prevention of type 2 diabetes mellitus: the STOP-NIDDM randomised trial. *Lancet (London, England)* **359,** 2072–7 (2002).
4. Van de Laar, F. A., Lucassen, P. L., Akkermans, R. P., Van de Lisdonk, E. H. & De Grauw, W. J. Alpha-glucosidase inhibitors for people with impaired glucose tolerance or impaired fasting blood glucose. *Cochrane Database Syst. Rev.* (2006), issue 4, CD005061
5. Schnell, O., Mertes, G. & Standl, E. Acarbose and metabolic control in patients with type 2 diabetes with newly initiated insulin therapy. *Diabetes, Obes. Metab.* **9,** 853–858 (2007).
6. Blaak, E. E. *et al.* Impact of postprandial glycaemia on health and prevention of disease. *Obes. Rev.* **13,** 923–984 (2012).
7. Lafiandra, D., Riccardi, G. & Shewry, P. R. Improving cereal grain carbohydrates for diet and health. *J. Cereal Sci.* **59,** 312–326 (2014).
8. Ray, K. Sen & Singhania, P. R. Glycemic and insulinemic responses to carbohydrate rich whole foods. *J. Food Sci. Technol.* **51,** 347–352 (2014).
9. Boers, H. M. *et al.* Efficacy of fibre additions to flatbread flour mixes for reducing post-meal glucose and insulin responses in healthy Indian subjects. doi:10.1017/S0007114517000277
10. Boers, H. M. *et al.* Efficacy of different fibres and flour mixes in South-Asian flatbreads for reducing post-prandial glucose responses in healthy adults. *Eur. J. Nutr.* **56,** 2049–2060 (2017).
11. Ohashi, Y. *et al.* Consumption of partially hydrolysed guar gum stimulates Bifidobacteria and butyrate-producing bacteria in the human large intestine. *Benef. Microbes* **6,** 451–455 (2015).
12. Papathanasopoulos, A. & Camilleri, M. Dietary fiber supplements: effects in obesity and metabolic syndrome and relationship to gastrointestinal functions. *Gastroenterology* **138,** 65-72.e1–2 (2010).
13. den Besten, G. *et al.* Protection against the metabolic syndrome by guar gum-derived short-chain fatty acids depends on peroxisome proliferator-activated receptor γ and glucagon-like peptide-1. *PLoS One* **10,** e0136364 (2015).
14. Grundy, M. M.-L. *et al.* Re-evaluation of the mechanisms of dietary fibre and implications for macronutrient bioaccessibility, digestion and postprandial metabolism. *Br. J. Nutr.* **116,** 816–833 (2016).
15. Osorio-Díaz, P., Agama-Acevedo, E., Mendoza-Vinalay, M., Tovar, J. & Bello-Pérez, L. A. Pasta added with chickpea flour: Chemical composition, in vitro starch digestibility and predicted glycemic index. *Cienc. y Tecnol. Aliment.* **6,** 6–12 (2008).
16. Jukanti, A. K., Gaur, P. M., Gowda, C. L. L. & Chibbar, R. N. Nutritional quality and health benefits of chickpea (Cicer arietinum L.): a review. *Br. J. Nutr.* **108,** S11–S26 (2012).
17. Ekström, L. M. N. K., Björck, I. M. E. & Östman, E. M. On the possibility to affect the course of glycaemia, insulinaemia, and perceived hunger/satiety to bread meals in healthy volunteers. *Food Funct.* **4,** 522–529 (2013).
18. Eelderink, C. *et al.* The glycemic response does not reflect the In vivo starch digestibility of fiber-rich wheat products in healthy men. *J. Nutr* **142,** 258–263 (2012).
19. Boers, H. M. *et al.* Effect of fibre additions to flatbread flour mixes on glucose kinetics: a randomised controlled trial. *Br. J. Nutr.* **118,** 777–787 (2017).
20. Trezzi, J.-P. *et al.* LacaScore: a novel plasma sample quality control tool based on ascorbic acid and lactic acid levels. *Metabolomics* **12,** 96 (2016).

21. Krämer, L., Jäger, C., Trezzi, J.-P., Jacobs, D. M. & Hiller, K. Quantification of Stable Isotope Traces Close to Natural Enrichment in Human Plasma Metabolites Using Gas Chromatography-Mass Spectrometry. *Metabolites* (2018). doi:10.3390/metabo8010015

22. Hiller, K. *et al.* Metabolite detector: Comprehensive analysis tool for targeted and nontargeted GC/MS based metabolome analysis. *Anal. Chem.* **81,** 3429–3439 (2009).

23. Jennings, M. E. & Matthews, D. E. Determination of complex isotopomer patterns in isotopically labeled compounds by mass spectrometry. *Anal. Chem.* **77,** 6435–6444 (2005).

24. Trezzi, J.-P. *et al.* Distinct metabolomic signature in cerebrospinal fluid in early parkinson's disease. *Mov. Disord.* **32,** 1401–1408 (2017).

25. Yuan, Y., Hoon Yang, T. & Heinzle, E. 13C metabolic flux analysis for larger scale cultivation using gas chromatography-combustion-isotope ratio mass spectrometry. *Metab. Eng.* **12,** 392–400 (2010).

26. Benjamini, Y. & Hochberg, Y. Controlling the false discovery rate: a practical and powerful approach to multiple testing. *Journal of the Royal Statistical Society. Series B (Methodological)* **57,** 289–300 (1995).

27. Marquardt, D. W. An algorithm for least-squares estimation of nonlinear Parameters. *J. Soc. Ind. Appl. Math.* **11,** 431–441 (1963).

28. Levenberg, K. A method for the solution of certain non-linear problems in least squares. *Q. Appl. Math.* **2,** 164–168 (1944).

29. Cavanaugh, J. E. Unifying the derivations for the Akaike and corrected Akaike information criteria. *Stat. Probab. Lett.* **33,** 201–208 (1997).

30. Grabacka, M., Pierzchalska, M., Dean, M. & Reiss, K. Regulation of ketone body metabolism and the role of PPARα. *Int. J. Mol. Sci.* **17,** (2016).

31. Krug, S. *et al.* The dynamic range of the human metabolome revealed by challenges. *FASEB J.* **26,** 2607–2619 (2012).

32. Moazzami, A. A., Shrestha, A., Morrison, D. A., Poutanen, K. & Mykkänen, H. Metabolomics reveals differences in postprandial responses to breads and fasting metabolic characteristics associated with postprandial insulin demand in postmenopausal women. *J. Nutr.* **144,** 807–814 (2014).

33. Pellis, L. *et al.* Plasma metabolomics and proteomics profiling after a postprandial challenge reveal subtle diet effects on human metabolic status. *Metabolomics* **8,** 347–359 (2012).

34. Fiamoncini, J. *et al.* Plasma metabolome analysis identifies distinct human metabotypes in the postprandial state with different susceptibility to weight loss–mediated metabolic improvements. *FASEB J.* fj.201800330R (2018). doi:10.1096/fj.201800330R

35. Van Der Borght, A., Goesaert, H., Veraverbeke, W. S. & Delcour, J. A. Fractionation of wheat and wheat flour into starch and gluten: overview of the main processes and the factors involved. *J. Cereal Sci.* **41,** 221–237 (2005).

36. Rombouts, I. *et al.* Wheat gluten amino acid composition analysis by high-performance anion-exchange chromatography with integrated pulsed amperometric detection. *J. Chromatogr. A* **1216,** 5557–5562 (2009).

37. Levitt, D. G. & Levitt, M. D. A model of blood-ammonia homeostasis based on a quantitative analysis of nitrogen metabolism in the multiple organs involved in the production, catabolism, and excretion of ammonia in humans. *Clin. Exp. Gastroenterol.* **11,** 193–215 (2018).

38. Adeva, M. M., Souto, G., Blanco, N. & Donapetry, C. Ammonium metabolism in humans. *Metabolism.* **61,** 1495–1511 (2012).

39. Nie, C., He, T., Zhang, W., Zhang, G. & Ma, X. Branched Chain Amino Acids: Beyond Nutrition Metabolism. *Int. J. Mol. Sci.* **19,** (2018).

40. Darmaun, D., Matthews, D. E. & Bier, D. M. Glutamine and glutamate kinetics in humans. *Am. J. Physiol.* **251,** (1986).

41.   Ferrannini, E. *et al.* Early metabolic markers of the development of dysglycemia and type 2 diabetes and their physiological significance. *Diabetes* **62,** 1730–1737 (2013).

42.   Foster, J. D. M. and D. W. Regulation of hepatic fatty acid oxidation and ketone body production. *Ann. Rev. Biochem.* **49,** 395–420 (1980).

43.   Yang, R. D., Matthews, D. E., Bier, D. M., Wen, Z. M. & Young, V. R. Response of alanine metabolism in humans to manipulation of dietary protein and energy intakes. *Am. J. Physiol.* **250,** E39-46 (1986).

44.   Eelderink, C. *et al.* Slowly and rapidly digestible starchy foods can elicit a similar glycemic response because of differential tissue glucose uptake in healthy men. *Am. J. Clin. Nutr.* **96,** 1017–1024 (2012).

45.   Adibi, S. A., Gray, S. J. & Menden, E. The kinetics of amino acid absorption and alteration of plasma composition of free amino acids after intestinal perfusion of amino acid mixtures. *Am. J. Clin. Nutr.* **20,** 24–33 (1967).

46.   Adibi, S. A. & Gray, S. J. Intestinal absorption of essential amino acids in man. *Gastroenterology* **52,** 837–845 (1967).

47.   Webb, K. E. Intestinal absorption of protein hydrolysis products: a review. *J. Anim. Sci.* **68,** 3011–22 (1990).

48.   Baxter, C. J., Liu, J. L., Fernie, A. R. & Sweetlove, L. J. Determination of metabolic fluxes in a non-steady-state system. *Phytochemistry* **68,** 2313–2319 (2007).

49.   Binsl, T. W. *et al.* Measuring non-steady-state metabolic fluxes in starch-converting faecal microbiota in vitro. *Benef. Microbes* **1,** 391–405 (2010).

50.   Dario Frias, A. C. & Sgarbieri, V. C. Guar gum effects on food intake, blood serum lipids and glucose levels of Wistar rats. *Plant Foods Hum. Nutr.* **53,** 15–28 (1998).

51.   Mariotti, F., Pueyo, M. E., Tomé, D., Benamouzig, R. & Mahé, S. Guar gum does not impair the absorption and utilization of dietary nitrogen but affects early endogenous urea kinetics in humans. *Am. J. Clin. Nutr.* **74,** 487–493 (2001).

52.   Rochus, K. *et al.* Highly viscous guar gum shifts dietary amino acids from metabolic use to fermentation substrate in domestic cats. *Br. J. Nutr.* **109,** 1022–1030 (2013).

53.   Katz, J., Lee, W. N. P., Wals, P. A. & Bergner, E. A. Studies of glycogen synthesis and the Krebs cycle by mass isotopomer analysis with [U-13C] glucose in rats. J. Biol. Chem. 264, 12994–13001 (1989).

Supplemental Table 1. Computed appearance rates for the three conditions, control, GG2 and GG4 and all 12 subjects separately

| Intervention	Subject	Glc_M6	Lac_M3	Ala_M3	Cit_M2	Glu_M2	Ser_M3	Gly_M2	Glu_M5	Gln_M5	Val_M5	Tyr_M9	Ile_M6	Lys_M6	Thr_M4
Ctrl	S01	SD>20%	0.0112444	0.00262465	0.000696408	0.000680515	0.004307	0.00283383	0.00460096	0.00502024	0.00421803	0.00609116	0.00368398	0.00494034	0.00362697
Ctrl	S02	0.0216101	0.00198953	0.000292416	0.000161624	0.00042625	0.000261194	0.000528255	0.000740867	0.000317899	0.000184817	SD>20%	SD>20%	SD>20%	0.000328045
Ctrl	S03	0.0489334	0.00464959	0.0015791	0.000468958	0.00148774	0.0031427	0.00173496	0.00333826	0.00421452	0.00217325	0.00421349	0.00328979	SD>20%	0.00254647
Ctrl	S04	0.0416053	0.00491107	0.00126395	0.000167461	0.00030312	0.000456815	0.000980747	0.00152231	0.00147087	0.000574341	0.00204836	0.00198461	SD>20%	0.00101638
Ctrl	S05	0.0883171	0.00401469	0.00111796	0.000715179	0.000200243	0.0048263	0.00188476	0.00326771	0.0361183	0.0025803	0.00401154	0.00258209	0.00651109	0.00339513
Ctrl	S06	0.0534804	0.00534168	0.000538422	0.000141413	0.000509664	SD>20%	0.000662765	0.00209619	0.0026769	SD>20%	0.00269476	0.0012342	0.00170872	SD>20%
Ctrl	S07	0.045238	0.00463571	0.00107515	0.000533714	0.000538809	0.000922512	0.00148207	0.00329265	0.0037606	0.00193248	0.00299281	0.0018179	0.00175688	SD>20%
Ctrl	S08	0.0244294	0.00289098	0.000610366	6.21932E-05	0.000215949	6.89005E-05	0.000532498	0.0010457	0.00107765	SD>20%	0.00116221	0.00106525	2.16657E-05	0.00011259
Ctrl	S09	0.0601249	0.00517463	0.000951125	0.000185678	0.000142302	0.00199629	0.00205412	0.00366407	0.00310469	0.00291518	0.00232911	0.00162569	0.0011449	SD>20%
Ctrl	S10	0.0535331	0.00579792	0.0010077	0.000300234	0.000345176	0.000833085	0.0016219	0.00254491	0.00236714	0.0010729	0.002299	0.00238175	0.000518488	0.00298898
Ctrl	S11	0.0456823	0.0500393	0.000869612	0.000137349	0.000368048	0.000702107	0.00105177	0.000865834	0.00129186	SD>20%	5.04619E-05	0.00138391	SD>20%	0.00047807
Ctrl	S12	0.0734951	0.00898923	0.00139439	0.000301233	0.000433943	0.00279261	0.00184818	0.00486607	0.00429717	0.00412804	0.00132503	0.00138758	SD>20%	0.00161698
GG2	S01	0.0523737	0.000239864	0.00125598	0.000147718	0.00020336	0.00202357	0.00238145	0.00288619	0.00317483	0.00164683	0.00400935	0.00432731	0.0021257	0.00270143
GG2	S02	0.0311704	0.00448961	0.00041878	0.000208552	SD>20%	7.65659E-05	0.000613232	0.000560846	0.00109883	0.000256772	0.000483072	SD>20%	0.000323628	0.000379571
GG2	S03	0.0364802	0.00394953	0.00132789	0.000351083	0.00197943	0.00402603	0.00149977	0.00279893	0.00343276	0.00207239	0.0043548	0.00329738	0.473528	0.00382618
GG2	S04	0.0253333	0.00476949	0.00155224	0.000364319	0.000227518	SD>20%	0.00117316	0.00259784	0.00188869	0.00110594	0.00210799	0.00155626	0.00322745	0.00155459
GG2	S05	0.0501106	0.00420263	0.000738893	6.8408E-05	0.000437241	0.0019941	0.000881825	0.00161744	0.00170311	0.000714276	0.0023495	0.00187123	0.00550075	0.000773598
GG2	S06	0.0223862	0.00381559	0.000670712	0.000115076	0.0001815	0.000911344	0.000329942	0.000512947	SD>20%	SD>20%	SD>20%	0.000103349	0.00270728	0.00289511
GG2	S07	0.0275109	0.00464659	0.000998753	0.000227652	0.000277003	0.00154323	0.0018764	0.00318697	0.00358752	0.00188899	0.0029159	0.00247462	SD>20%	0.00294037
GG2	S08	0.0327049	0.00239974	0.000520805	0.000227408	0.000286279	0.000196239	SD>20%	0.00122859	0.000914224	0.00816178	3.27185E-05	0.00118579	2.53487E-05	0.00280695
GG2	S09	0.047741	0.00584255	0.00137517	0.000244413	0.00032763	0.00182977	0.00231787	0.00241928	0.00394024	0.00458822	SD>20%	0.00185087	0.00386999	0.00384265
GG2	S10	0.0569686	0.0037049	0.00120338	0.000170248	0.000582631	0.00217222	0.00141919	0.00244326	0.00282444	0.00145945	0.00248561	0.0033943	SD>20%	0.00287086
GG2	S11	0.0205617	0.00300231	0.000420249	0.000169283	0.000217321	0.000166934	0.000422364	0.000273486	0.000262408	0.000164824	2.33659E-05	SD>20%	0.00161417	6.24625E-05
GG2	S12	0.0618062	0.00549735	0.0011197	0.000343609	0.00016031	0.0019286	0.00176046	0.00342178	0.00339553	0.00227288	0.00141687	0.00150731	SD>20%	SD>20%
GG4	S01	SD>20%	0.00537414	0.00113245	0.000455461	0.00081278	0.00133719	SD>20%	0.00409075	0.00423424	0.00250547	0.0040532	0.00192305	0.00323156	0.00273187
GG4	S02	0.021533	0.00280937	0.000343153	9.8585E-05	0.000306804	0.000299762	0.000467464	0.000672448	0.000523637	0.000172769	0.000160148	0.000205187	0.00227658	0.000425093
GG4	S03	0.0217631	0.00307338	0.000741115	0.000169458	0.000357652	0.00153308	0.000790021	0.00150865	0.00258865	0.000596121	0.00148884	0.00266906	0.00544026	0.00113151
GG4	S04	0.0234766	0.00409712	0.000985566	7.79388E-05	0.000227597	0.000486434	0.000818047	SD>20%	0.00176826	0.000385256	0.000775104	0.000459319	0.00114691	0.000927679
GG4	S05	0.0689647	0.00426395	0.00113879	0.000539565	0.000547669	0.00334107	0.0019548	0.00275928	0.00434717	0.00620099	0.00453314	0.00276509	0.003296	0.00338823
GG4	S06	0.0223743	0.00243835	0.00411013	9.0749E-05	0.00019309	0.000238407	0.000604515	0.000734459	0.00346807	0.00377028	0.000588637	SD>20%	0.0012489	0.00130013
GG4	S07	0.0310916	0.00537583	0.000794677	0.000356699	0.000358186	0.000546199	0.00107165	0.00269956	0.00236664	0.00174713	0.00218904	0.00328834	0.00105075	0.0058185
GG4	S08	0.0253347	0.00461788	0.000734632	0.00014219	0.000330079	0.00201852	0.00208368	0.0017767	0.00209573	0.000980964	SD>20%	0.00207974	SD>20%	0.00178079
GG4	S09	0.0403291	0.00474064	0.000962051	0.00014366	0.000265582	SD>20%	0.0015761	0.00323441	0.00261923	0.00343392	0.00269295	0.000746243	0.00131859	SD>20%
GG4	S10	0.0316682	0.00327989	0.00087145	0.000396567	0.000327481	0.000746499	0.0013722	0.00163245	0.00138484	0.000918844	0.0021790	0.00238629	0.00293585	SD>20%
GG4	S11	0.016532	0.00211756	0.000436068	0.000147693	6.11436E-05	0.000266185	SD>20%	0.000199415	0.000197782	0.000115482	0.000114918	SD>20%	SD>20%	SD>20%
GG4	S12	0.021323	0.00441071	0.000651871	0.000185155	0.000134324	SD>20%	0.000339075	0.000892658	0.000305311	0.000240027	SD>20%	SD>20%	SD>20%	2.4789E-05
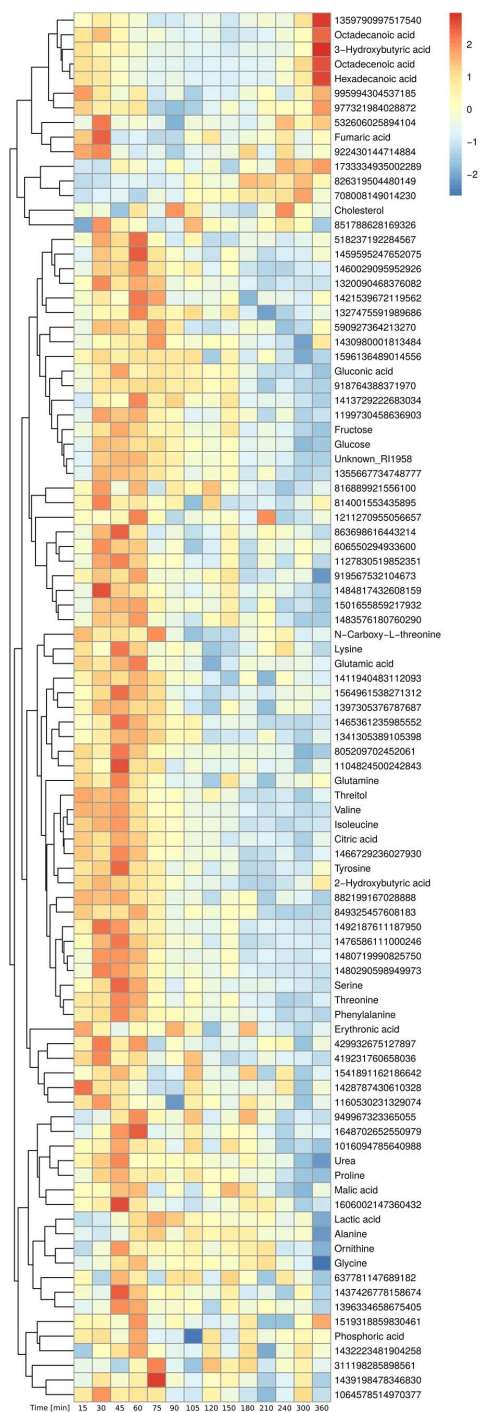
Supplemental Figure 1: Postprandial effect of wheat bread intake – Heatmap of significantly changed metabolites over time (Median of all subjects, Baseline correction, zScore Normalization
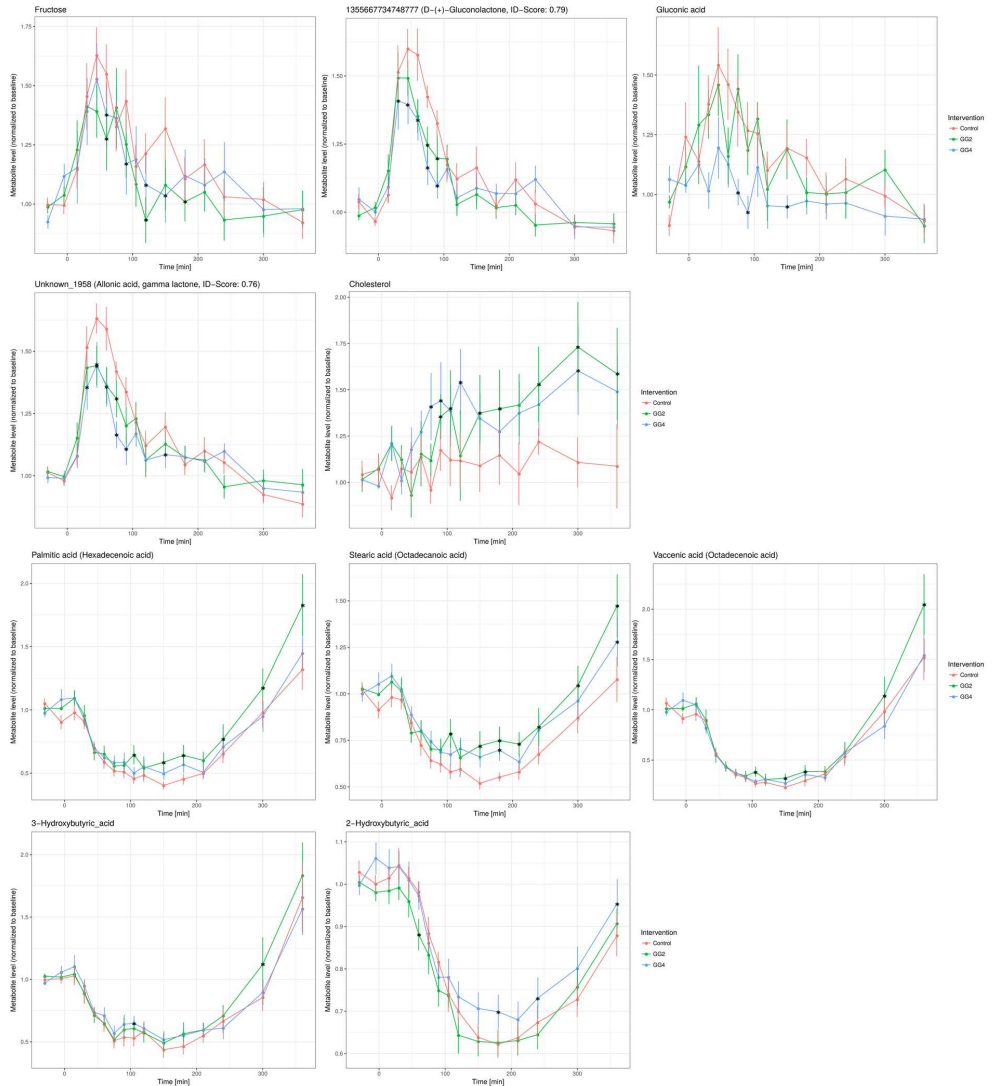
Supplemental figure 2: Significantly altered metabolite level profiles upon intervention for Fructose, 1355667734748777 (putative Gluconolactone), Gluconic acid, unknown_1958 (putative Allonic acid gamma lactone), Cholesterol and palmitic acid, stearic acid, vaccenic acid, 3-hydroxybutyric acid and 2-hydroxybutyric acid
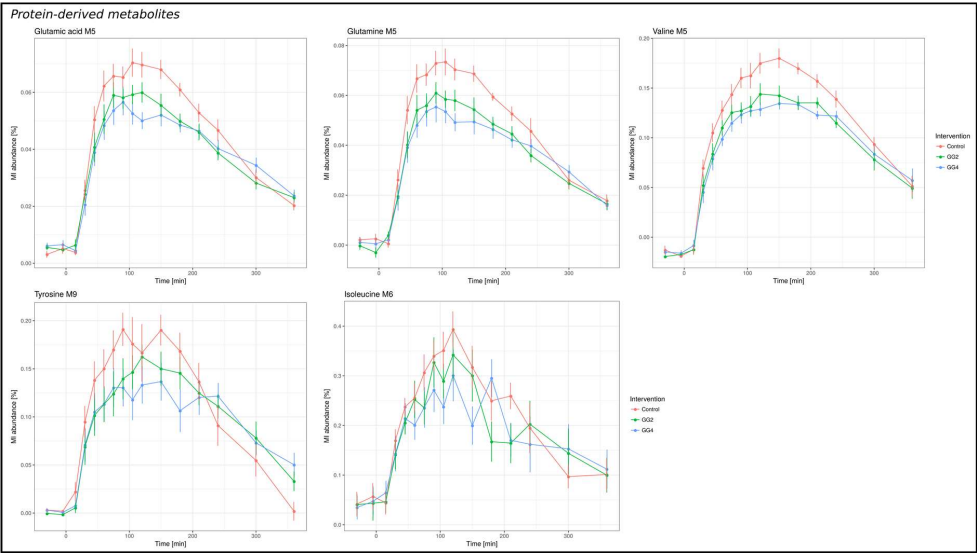
Supplemental Figure 3. Response curves of ^{13}C-enrichment profiles over time upon intervention for protein-derived metabolites: glutamic acid M5, glutamine M5, valine M5, tyrosine M9, isoleucine M6 (Red – Control, Green – GG2, Blue – GG4; Average of MI abundance in % ± standard error of 12 subjects)